Effect of Surface Treatment of Fuel Cladding on Crud Deposition and Its General Corrosion

Hee-Sang Shim[1,*], Seung Heon Baek[2], Do Haeng Hur[1]
[1]*Materials Safety Technology Development Division, KAERI, 989-111 Daedeok-daero, Yuseong-gu, Daejeon 34057, Korea*
[2]*Future & Challenge for Clean Nuclear Energy, Heungdeok 1-ro, Giheung-gu, Yongin-Si, Gyeonggi-do, 16954, Korea*
**Corresponding author: hshim@kaeri.re.kr*

1. Introduction

The sub-cooled nucleate boiling (SNB) on fuel cladding surface is the driving force for crud deposition, which have often caused fuel integrity problems such as crud-induced power shift and crud-induced localized corrosion [1, 2]. The SNB as a heat transport mechanism is defined as the phenomenon in which bubbles formed on a heated surface take off into the coolant and disappear with heat transfer. In general, this is affected by the temperature difference between heated surface and coolant, and by the surface state of materials [3,4]. Thus, surface modification of fuel cladding has been studied by some research groups as a method to decrease the amount of fuel crud deposits [5-7].

In our previous work, we also reported that chemical etching of fuel cladding surface can dramatically reduce crud deposition due to reduction in SNB events and improvement in water contact angle, as shown Fig. 1 [5].

In this study, we investigated the oxidation rate of fuel cladding for 10,000 hours with and without chemical etching, respectively, and comparatively analyzed their oxide films, in order to evaluate the effect of chemical surface treatment of fuel cladding on fuel integrity.

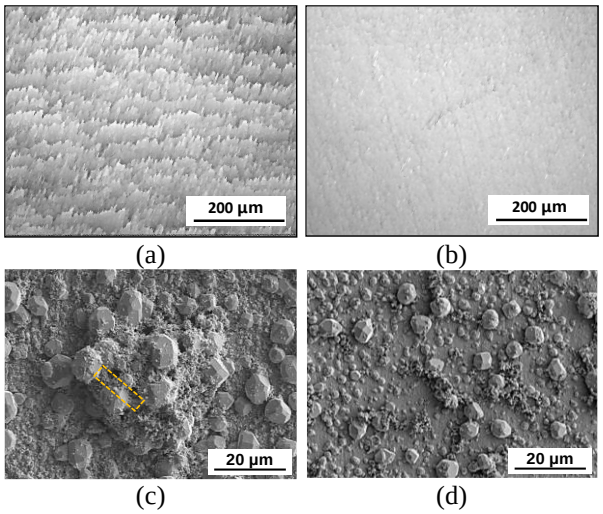

Fig. 1 Three-dimensional surface profiles (a, b) and Top-view morphologies of crud deposited in primary water condition (c, d); (a,c) as-received and (b,d) chemically-etched specimens.

2. Experimental

Zirconium base alloy tube, which has the same properties with commercial fuel cladding tube, Zirlo, was used as a test specimen as shown in table 1. The dimensions of the test cladding tubes were an outer diameter (OD) of 9.5 mm, and inner diameter (ID) of 8.3 mm. We prepared two types of tube specimens etched chemically and not. Before chemical etching, the tube specimens were cut to a length of 2 mm and 12 pieces were prepared. The as-received (AR) specimens were also prepared with 12 pieces.

The chemically etched (CE) cladding tube was prepared through immersion in an acid solution composed of 45 vol% nitric acid (65%-HNO_3), 5 vol% hydrofluoric acid (48%-HF), and 50 vol% deionized water for 3 min at room temperature. After the chemical etching, the cladding tube was rinsed immediately in deionized water for 10 min using an ultrasonic cleaner to avoid staining of the surface with the residual etching chemicals.

To carry out the corrosion test, all prepared specimens were pre-characterized by weight and surface area before the test was initiated. The surface area was carefully measured for each specimen by measuring the dimensions of specimen, such as ID and OD, length and wall thickness as well as excluding the holes drilled, using a digital Vernier caliper. The specimens pre-characterized were sequentially degreased in acetone, alcohol and deionized water for 10 min each.

The corrosion test was performed according to the procedure of ASTM G2/G2M-19[8], which is a standard evaluation method for zirconium and its alloys. Prior to test, the autoclave with a volume of 3.75 L and specimen tree, which were constructed with stainless 316L, were pre-conditioning in deionized water at 360°C for one week after cleaning. After pre-conditioning was completed, the specimens were hung at specimen tree and it was inserted into the autoclave. The deionized water was filled in the autoclave and it was purged with argon gas for 24 hours after covering its lid, to eliminate the dissolved oxygen. Then, the autoclave was gradually heated until the temperature of coolant reached to 360°C. In addition, the weigh measurement of the specimens was performed with 500 hours intervals for 10,000 hours to evaluate the corrosion rate.

The morphology and thickness of the oxidation layer for some sampled specimens was analyzed using scanning electron microscope (SEM) equipped with focused ion beam (FIB) machine. In addition, the crystallography of the oxidized specimens was analyzed using X-ray diffraction (XRD). The composition profiles of the oxidized specimens in cross-sectional view were measured using the energy dispersive spectroscopy (EDS) equipped with transmission

electron microscope (TEM). Furthermore, the surface zeta potential of as-prepared and oxidized specimens was measured for discussing the reason of change in crud deposition on two-types cladding tubes.

Table 1. Chemical composition and mechanical properties of Zr alloy cladding tube

Chemical composition (wt%)				
Sn	Fe	O	Nb	Zr
1.0	0.1	0.12	1.0	Bal.

Mechanical properties (at RT)		
YS (MPa)	UTS (MPa)	Elong. (%)
612.5	819.2	15.8

3. Results and discussion

Fig. 2 shows the weight gain of fuel cladding materials including AR and CE specimens tested by ASTM G2/G2M. AR and CE specimens show similar result in weight gain during corrosion test for 10,000 hours as shown in Fig.2(a). This is similar trend with the result for Zirlo tubing, which was evaluated using the same method, in other literature [9], as shown in Fig. 2(b).

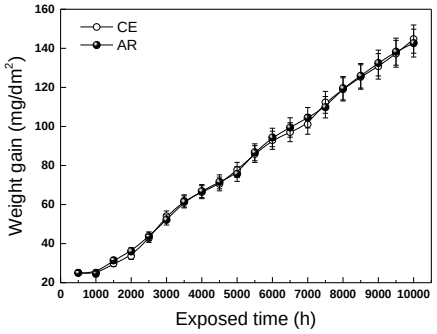

(a)

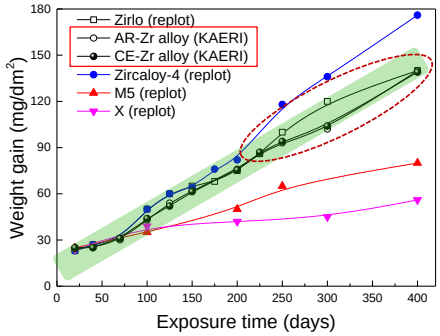

(b)

Fig. 2 Weight gain of (a) as-received and chemically-etched specimens evaluated through corrosion test for 10,000 hours, and (b)comparison with literature [9].

Fig. 3 displays the cross-sectional SEM images of oxidation layer of AR and CE specimens corroded for 500, 4,000 and 10,000 hours. Thickness of oxide layer increased as a function of test time in both of AR and CE specimens. In addition, the oxide layer corroded for 500 hours seems very dense as shown in Figs. 3(a) and 3(b). However, although no significant differences can be found between AR and CE specimens, a lot of cracks were observed in the oxide layer corroded for 4,000 and 10,000 hours. Furthermore, the crack length and density increased as the test time increased as shown in Figs. 3(c) to 3(f).

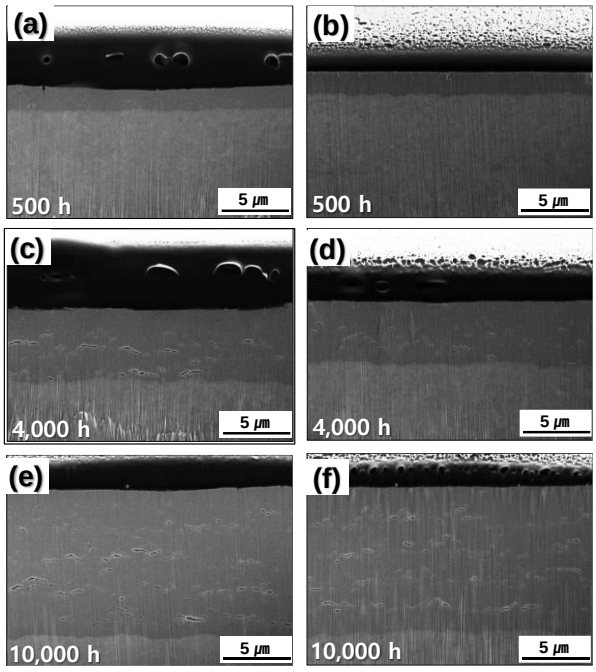

Fig. 3 Cross-sectional SEM images of specimens corroded for 500, 4,000, and 10,000 hours; (a, c, e) AR cladding and (b,d, f) CE cladding.

Fig. 4 shows the XRD patterns of AR and CE specimens as the test time increases. The characteristic peaks of metallic Zr-1.0Nb, which is referred to JCPDS No. 05-0665, were observed on AR and CE specimens corroded for 500 and 2,000 hours. In addition, the characteristic peaks of Zr-1.0Nb disappeared and the characteristic peaks of monoclinic zirconium dioxide (m-ZrO_2), which is referred to JCPDS No. 37-1484. The intensity of the m-ZrO_2 characteristic peaks gradually increased as the test time increased in the range of 4,000 to 10,000 hours. However, no difference between AR and CE specimens was also observed in XRD results.

The zirconium content in oxide layers of both AR and CE specimens gradually increased from water-side to metal-side in TEM-EDS results as shown in Fig. 5. While the oxygen content in oxide layers gradually decreased from water-side to metal-side.

Fig. 6 shows the surface zeta potentials between AR, CE, oxidized-AR, oxidized-CE and magnetite (Fe_3O_4) particle. The surface zeta potentials between AR and CE specimens, and between those oxidized specimens displays worthful differences. The zeta potential difference between CE specimen and Fe_3O_4 particle was larger by 2.3 mV than that between AR specimen and Fe_3O_4 particle. This characteristic was observed on the surface their oxidized surface. In other words, the

repulsive force between CE surface and Fe_3O_4 particle is larger than between AR surface and Fe_3O_4 particle.

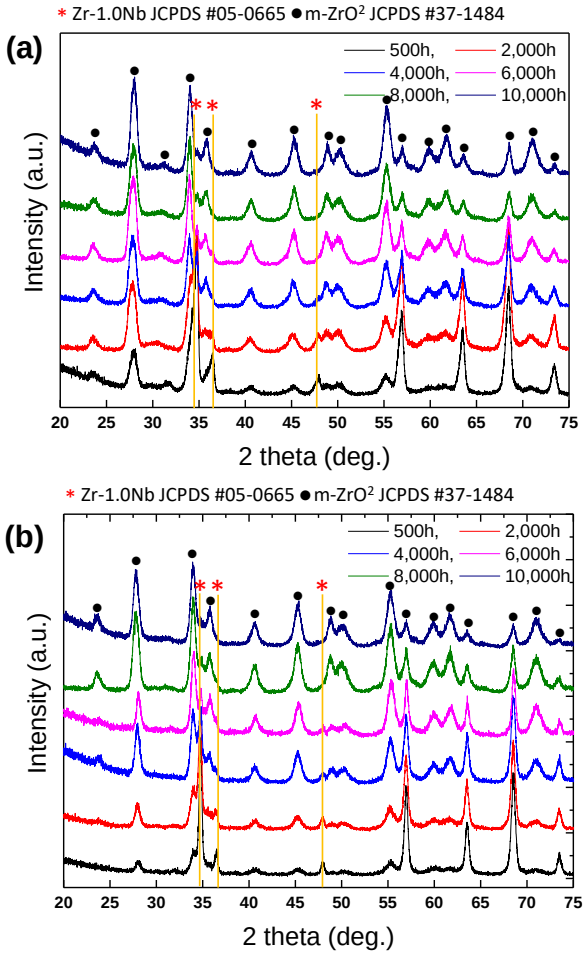

Fig. 4 XRD patterns of oxidized specimens as the test time increased; (a) AR cladding and (b) CE cladding.

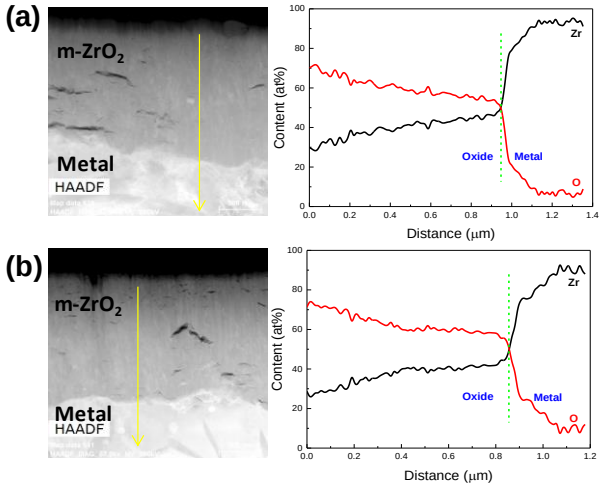

Fig. 5 STEM image and EDS profiles; (a) AR cladding and (b) CE cladding.

Considering analyzed results for oxide layers, AR and CE specimens shows no difference in oxidation behaviors such as weight gain, morphology and crystallography of oxide layer. In addition, the change in chemical composition from water-side to metal-side might be caused by diffusion limitation of oxygen content in internal oxidation process. However, the surface zeta potential between cladding surface and Fe_3O_4 particle might be important factor along with SNB event and water contact angle. Therefore, the chemical treatment of cladding surface can be utilized as a method to reduce dramatically crud deposit on it without negative effect on cladding oxidation.

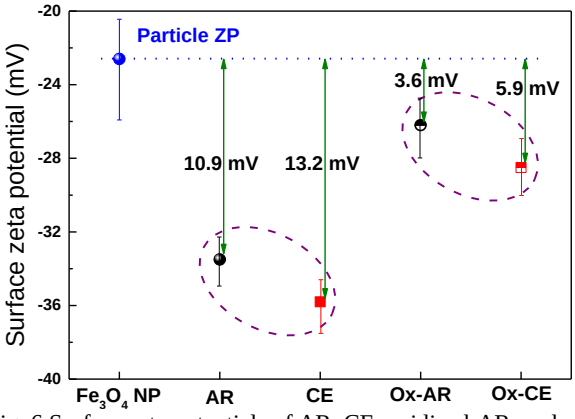

Fig. 6 Surface zeta potentials of AR, CE, oxidized-AR, and oxidized-CE with particle zeta potential of magnetite.

4. Conclusions

We have investigated the oxidation behaviors of CE cladding, which has shown the dramatic reduction of crud deposition in PWR primary condition. As a result, no difference was observed in oxidation characteristics such as weight gain, crystallography, oxide morphology, its chemical composition, and etc. from AR cladding. However, the surface zeta potential between cladding surface and Fe_3O_4 particle shows worthful difference for oxidized surface as well as as-received surface. The CE and its oxidized surfaces have large repulsive pulse with corrosion product particles, which can be possible to mitigate crud deposition. Therefore, it is believed that the chemical etching technology of fuel cladding will be possible to prohibit crud problem in PWRs.

Acknowledgments

This study was supported by the National Research Foundation (NRF) grant funded by the government of the Republic of Korea (grant number RS-2022-00143316).

REFERENCES

List and number all bibliographical references in 9-point Times, single-spaced, at the end of your paper. When referenced in the text, enclose the citation number in square brackets, for example [1]. It is recommended that the number of references does not exceed five.

[1] J. Deshon, D. Hyssey, B. Kedrick, J. McGurk, J. Secker, and M. Short, Pressurized Water Reactor Fuel crud and corrosion modeling Nuclear Reactor Power Monitoring, Journal of Materials, 2011.
[2] D. Hussey, D. Wells, Fuel Reliability Guidelines: PWR Fuel Cladding Corrosion and Crud, Rev.1, EPRI Report 3002002795, Palo Alto, EPRI, .2014.
[3] S. Odar, Crud in PWR/VVER Coolant, Vol.1 – Sources, Transportation in Coolant, Fuel Deposition and Radiation Build-up, A.N.T Int'l, 2014.
[4] J. Deshon, PWR Axial Offset Anomaly (AOA) Guidelines, Rev.1, EPRI Reprot 1008102, Palo Alto, EPRI, 2004.
[5] S. H. Baek, H. -S. Shim, J. G. Kim, D. H. Hur, Effect of chemical etching of fuel cladding surface on crud deposition behavior in simulated primary water of PWRs at 328oC, Annals Nucl. Ener. 116(2018) 69-77.
[6] H.-S. Shim, M.-S. Park, S. H. Baek, D. H. Hur, Effect of aluminum oxide coated on fuel cladding surface on crud deposition in simulated PWR Primary water, Annals Nucl. Ener. 121(2018) 607-614.
[7] E. Paramonova, Crud Resistant Fuel Cladding Materials, Thesis, MIT, 2013.
[8] ASTM G2/G2M-19, Standard Test Method for Corrosion Testing of Products of Zirconium, Hafnium, and Their Alloys in Water at 680ºF(360ºC) or in Steam at 750ºF(400ºC), 2020, ASTM.
[9] A. T. Motta, A. Couet, R. J. Comstock, Corrosion of Zirconium Alloys Used for Nuclear Fuel Cladding, Annu. Rev. Mater. Res. 45(2015) 311-343.